Response to the Comments from Reviewer #2:

Reviewer #2: This manuscript investigates the influence of El Niño and Tibetan Plateau snow cover on the winter $PM_{2.5}$ dipole pattern over China, using EOF analysis, statistical diagnostics, and CESM sensitivity experiments. The study links large-scale climate variability with regional air pollution and identifies a north-south dipole structure associated with atmospheric circulation changes. Overall, the manuscript is well organized, and the topic is quite interesting. However, several key issues related to experimental design, physical interpretation, and methodological consistency need to be addressed to improve the robustness and credibility of the conclusions.

Response:

- We would like to thank the reviewer very much for the positive and valuable feedback on our manuscript and providing us with suggestions and guidance. We have revised our manuscript to address your comments and suggestions, as illustrated below.

Major Comments:

The CESM sensitivity experiments are conducted for only a single winter period, which raises concerns about the robustness. Given the strong interannual variability of atmospheric circulation, it is recommended to include multi-year trials to enhance the reliability of the simulation results.

Response:

- We thank the reviewer for this valuable comment. We acknowledge that single-winter simulations are inherently limited in their ability to isolate forced responses from internal atmospheric variability. Our primary conclusions are based on statistical analysis based on observational and reanalysis data. The EOF decomposition, partial correlation analyses, and regression diagnostics are all performed on this long observational record, providing a statistically robust foundation for our findings. The CESM sensitivity experiments serve a complementary and confirmatory role, corroborating the directionality and physical plausibility of the identified mechanisms rather than precisely quantifying the magnitude of forced responses. To minimize interference from background climate variability, we selected the winter from November 2010 to February 2011. This period was characterized by neutral ENSO conditions and neutral TP snow anomalies, allowing the imposed albedo perturbations to be interpreted more clearly in isolation. We have revised the manuscript to explicitly state that the CESM experiments are designed as process-oriented sensitivity tests, and that their results are interpreted qualitatively in support of the statistical conclusions.

- **"To further verify the role of El Niño-like SST anomalies, sensitivity simulations were conducted by imposing warm SST anomalies associated with the Niño 1+2 index (Fig. A6). Fig. 5a shows the differences between the $CESM_{ElNiño}$ and $CESM_{ctrl}$ experiments, which isolate the atmospheric and $PM_{2.5}$ response to El Niño forcing. Consistent with the statistical analysis, the imposed El Niño-like SST pattern strengthens the western Pacific subtropical high, induces anomalous southerly winds over eastern China, and enhances moisture transport into southern China (Fig. A6a, b). Consequently, surface $PM_{2.5}$ concentrations decrease markedly in southern China, with reductions of approximately 12 μg m^{-3} over the Sichuan Basin and 6 μg m^{-3} over the Yangtze River Delta (Fig. 5a). In contrast, $PM_{2.5}$ concentrations increase slightly over northeastern China by about 3 μg m^{-3}, further confirming the El Niño-driven north-south dipole structure captured by EOF2."**

- **"To assess the causal impact of TP snow cover, we performed a targeted CESM experiment ($CESM_{TPSC}$) in which surface albedo over the northern TP (86°-94°E, 35°-40°N) was prescribed with a minimum value of 0.8. Surface albedo represents the reflectivity of the land surface, integrating contributions from all surface components including snow, soil, and vegetation. A minimum value of 0.8 was imposed to simulate persistent high snow cover conditions, consistent with the characteristically high reflectivity of snow-dominated surfaces (Cohen and Rind, 1991). The CESM results reproduce a coherent cooling response over the northern TP and a corresponding weakening of the subtropical westerly jet, which leads to increases in surface relative humidity and reductions in both planetary boundary layer height and near-surface wind speed over northern China (Fig. A6), supporting positive $PM_{2.5}$ anomalies over the BTH region (Fig. 5b). These modeled responses are consistent with the observational regression analysis, reinforcing the physical credibility of the identified snow-forcing mechanism."**

- **"While the CESM sensitivity experiments provide valuable process-level**

insight into the physical mechanisms linking TP snow cover and El Niño to $PM_{2.5}$ variability, several limitations warrant acknowledgment. The experiments are based on a single-winter simulation, which precludes a rigorous assessment of statistical significance in the presence of internal atmospheric variability. Accordingly, the model results are interpreted qualitatively as process-oriented sensitivity tests that corroborate the sign and directionality of the identified mechanisms, rather than as quantitative estimates of forced response magnitudes."

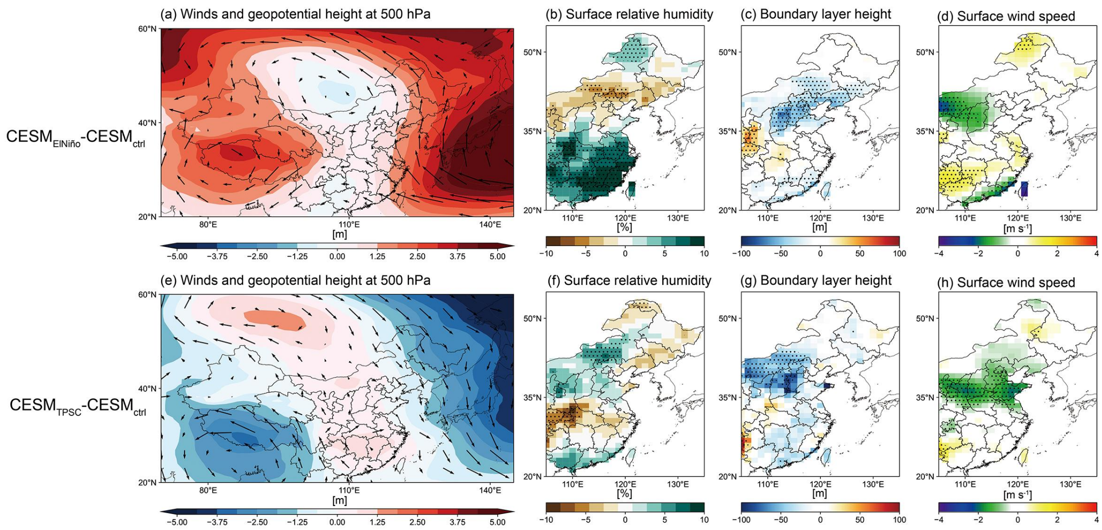

Figure A6. CESM simulated responses of (a, e) geopotential height (m, contour) and wind fields (m s^{-1}, vector) at 500 hPa, (b, f) surface relative humidity (%), (c, g) planetary boundary layer height (m) and (d, h) surface wind speed (m s^{-1}) during winter to Niño 1+2, and higher albedo forcing over the northern TP.

The second EOF mode (PC2), although central to the manuscript, explains a relatively limited fraction of variance and its physical interpretation is not sufficiently clarified. It remains unclear whether PC2 represents a dynamically independent mode or a statistical pattern resulting from multiple overlapping processes.

Response:

- We thank the reviewer for this insightful comment. The relatively smaller variance explained by EOF2 is expected because the dominant variability of $PM_{2.5}$ in China is strongly controlled by anthropogenic emissions, which are primarily represented by EOF1. Although EOF2 explains a relatively smaller fraction of the total variance (13.2%) compared with EOF1, it is well separated from higher-order modes according to the North test, indicating that the mode is statistically robust. EOF2 exhibits a north-south dipole structure accompanied by consistent meteorological anomalies, including anomalous circulation, moisture transport, precipitation, surface wind speed, and boundary layer height. These results suggest that EOF2 reflects a physically meaningful mode of climate-related $PM_{2.5}$ variability. We have clarified this point in the revised manuscript:

- **"EOF2, accounting for 13.2% of the total variance, reveals a pronounced north-south dipole pattern in winter $PM_{2.5}$ concentrations over eastern China, characterized by positive anomalies in northern China and negative anomalies in southern China. PC2 displays strong interannual variability, with predominantly negative values before 2012 and mainly positive values during 2013-2020. We examined the correlations between PC2 and anthropogenic SO_2 and NO_x emissions across eastern, northern, and southern China. The correlation coefficients between PC2 and SO_2 (NO_x) emissions are -0.41 (-0.01), -0.37 (0.07), and -0.43 (-0.11) in eastern, northern, and southern China, respectively. None of these correlations are statistically significant, and critically, they exhibit no north-south dipole structure that could mirror the EOF2 pattern. This confirms that the spatially heterogeneous emission controls do not drive the EOF2 dipole structure. To elucidate the meteorological conditions underlying the EOF2 dipole structure, regression maps of atmospheric circulation and meteorological fields onto the normalized PC2 are shown in Fig. 2. At the 500 hPa level, a pronounced anticyclonic circulation anomaly is observed over northeastern China and Japan, accompanied by a weaker cyclonic anomaly over the southern Tibetan Plateau. This configuration induces anomalous southerly flow across eastern China. In southern China, these southerly winds transport humid air from the South China Sea, enhancing precipitation by approximately 0.2 mm month^{-1} and promoting wet removal of $PM_{2.5}$. In contrast, over northern China, the southerly anomalies weaken atmospheric ventilation, as reflected by reduced surface wind speeds (-0.05 m s^{-1}) and a suppressed planetary boundary layer height (-30 m), favoring pollutant accumulation and increasing $PM_{2.5}$ levels. As a result, anomalous southerly flow exerts opposite influences on winter $PM_{2.5}$ concentrations in northern and southern China, which is consistent with previous findings (Zhang et al., 2022; An et al., 2022). These results confirm that EOF2 dipole pattern primarily reflects large-scale meteorological forcing rather than anthropogenic emission variability."**

The treatment of Tibetan Plateau snow cover raises concerns. The selected region is relatively limited and characterized by generally shallow and sparse snow cover, which may weaken its physical representativeness. In such regions, variations in snow cover fraction alone may not be sufficient to induce strong surface energy perturbations or atmospheric responses, and this issue is not sufficiently discussed. In addition, it should be noted that the temporal variability of snow cover differs markedly across different regions of the Tibetan Plateau. In contrast, previous studies suggest that snow anomalies over the whole Tibetan Plateau are more likely to generate large-scale circulation responses affecting eastern China. Therefore, the current regional definition may not fully capture the relevant physical processes.

Response:

- We thank the reviewer for this thoughtful comment and fully appreciate the concerns raised regarding the physical representativeness of the selected region. We address each point in turn.

- Regarding snow cover depth and sparsity, we calculated the snow cover extent over the northern Tibetan Plateau (86°-94°E, 35°-40°N) from observational data throughout 1979-2021, as shown in Figure A7(a). The results reveal pronounced interannual variability, with notably elevated values in recent years, demonstrating that snow cover over this region is by no means uniformly shallow or sparse, particularly in recent decades. Furthermore, the regression analysis demonstrates that snow anomalies over the northern TP are capable of inducing a pronounced cooling effect on the atmospheric column exceeding 5 W m^{-2}, which is of sufficient magnitude to modulate the subtropical westerly jet and drive the large-scale circulation anomalies over eastern China documented in Figure 7. This confirms that the surface energy perturbations associated with snow cover variability in this region are physically meaningful.

- Regarding the choice of the northern TP rather than the whole Tibetan Plateau, we acknowledge the reviewer's point that snow anomalies over the broader Tibetan Plateau may also drive large-scale circulation responses. We performed correlation and partial correlation analyses between PC2 and snow cover across the entire Tibetan Plateau. The results show that statistically significant correlations are confined to the northern TP subregion, whereas no significant relationship is found when using a domain-wide TP snow cover index. As the reviewer notes, snow cover variability differs markedly across different sub-regions of the Tibetan Plateau, and defining a single domain-wide index may offset the potential impact of of signals from different regions on atmospheric circulation. The use of a sub-regional snow cover index is therefore both statistically motivated and physically justified, and is consistent with previous studies that similarly defined sub-regional indices over specific portions of the Tibetan Plateau and demonstrated their influence on meteorological anomalies over China (e.g., Wang et al., 2021; Chen et al., 2021). These clarifications have been added to the revised manuscript.

- **"After excluding the ENSO signal, PC2 remains significantly correlated with snow cover over the northern TP (Fig. 3d), indicating that interannual variability in winter $PM_{2.5}$ over China is also modulated by TP snow anomalies. To quantify this relationship, we define a Tibetan Plateau Snow Cover (TPSC) index as the wintertime area-averaged snow cover over the northern TP (86°-94°E, 35°-40°N), described by the blue box in Fig. 3d. The TPSC index eassociated snow albedo xhibits pronounced interannual variability throughout 1979-2021, with notably elevated values in recent years (Fig. A7). The correlation coefficient between the Niño 1+2 index and the TPSC index is -0.28 ($p > 0.24$), indicating that the linear dependence between the two predictors is weak and statistically insignificant. To formally evaluate the degree of multicollinearity among PC2, Niño 1+2, and TPSC, we computed the Variance Inflation Factor (VIF) for each variable. The resulting VIF values are 1.87, 1.90, and 1.47, respectively, all well below the commonly adopted threshold of 5 (O'Brien, 2007), confirming that multicollinearity does not pose a meaningful threat to the robustness of the partial correlation results. Partial correlation analysis, with the ENSO signal removed, reveals a significant positive correlation between the TPSC index and PC2 ($r = 0.49$, $p < 0.05$). In contrast, no statistically significant relationship emerges when a domain-wide TP snow cover index is employed, suggesting that the dynamically relevant snow signal is regionally confined to the northern TP rather than reflecting a plateau-wide forcing."**

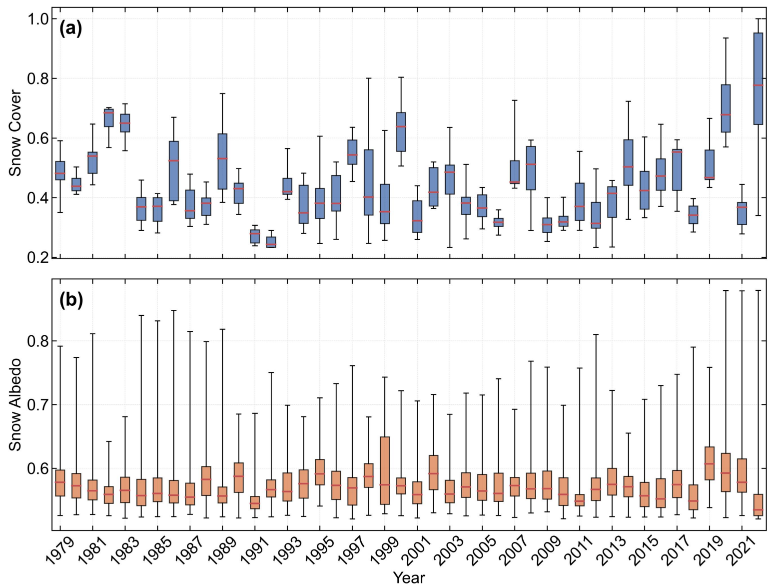

Figure A7. Interannual variations in winter (a) snow cover extent and (b) snow albedo over the northern Tibetan Plateau (86°-94°E, 35°-40°N) during 1979-2021. In each boxplot, the central red line denotes the median value, the box boundaries indicate the interquartile range (25th-75th percentiles), and the whiskers represent the minimum and maximum values.

The snow forcing experiment is highly idealized. Using a fixed high albedo (0.8) to represent enhanced snow cover deviates from realistic conditions, especially in regions where snow is typically thin. This setting may overestimate the snow-albedo effect and lacks representation of realistic snow processes and land-atmosphere interactions. The implications of this simplification should be more clearly discussed.

Response:

- We thank the reviewer for this constructive comment. The snow albedo over the northern Tibetan Plateau from reanalysis data for every winter from 1979 to 2021 were calculated in Figure A7(b). It exhibits substantial interannual variability, with maximum values frequently approaching or exceeding 0.8 in multiple years across the 1979-2021 period. Therefore, we believe the albedo of 0.8 is physically realistic. In the $CESM_{TPSC}$ experiment, when the model-simulated albedo falls below 0.8, it is reset to 0.8 to represent increased snow cover. Grid points where albedo already exceeds this threshold retain their original higher values, ensuring that the prescribed forcing reflects a physically plausible enhancement. We nonetheless fully acknowledge that this idealized design carries inherent limitations. By prescribing a fixed albedo floor rather than explicitly simulating snow depth, snow density, or snow melting processes, the experiment does not capture the full complexity of realistic snow-land-atmosphere interactions, including the insulating effect of snowpack on soil temperature, sublimation, and the feedback between snow cover and boundary layer turbulence. These processes could modulate the strength and spatial extent of the atmospheric response in ways that our experimental design cannot fully represent. It should be noted that the role of the $CESM_{TPSC}$ experiment in this study is confirmatory rather than quantitative. Such prescribed-albedo perturbations have been used to isolate the atmospheric response to snow cover anomalies in previous study (Wang et al., 2021). We have added a more explicit discussion of these limitations and their implications to the revised manuscript.

- **"$CESM_{TPSC}$, in which surface albedo over the northern Tibetan Plateau (86°-94°E, 35°-40°N) was set to a minimum of 0.8 to represent enhanced snow cover conditions (Cohen and Rind, 1991), following Wang et al. (2021). Specifically, when the model-simulated albedo falls below 0.8, it is reset to 0.8 to represent increased snow cover over the northern Tibetan Plateau. Grid points where albedo already exceeds this threshold retain their original values."**

- **"The idealized albedo perturbation in the $CESM_{TPSC}$ experiment does not explicitly simulate snow depth, density, or melting processes, which may lead to an overestimation of snow forcing strength compared to realistic conditions."**

Minor Comments:

The manuscript does not clearly distinguish between snow albedo and surface albedo over snow-covered areas. These represent different physical quantities, and clearer definitions would improve the interpretation of radiative processes.

Response:

- We thank the reviewer for this important clarification. In the regression analysis, we used snow albedo provided by ERA5, not surface albedo as previously stated. This error has been corrected throughout the manuscript. We have revised the manuscript to clearly distinguish between snow albedo and surface albedo:

- **"Fig. 6 illustrates anomalies in surface heat fluxes and the total atmospheric column heat source regressed onto the TPSC index. Enhanced snow cover over the northern TP increases snow albedo by approximately 0.02, leading to an increase in upward shortwave radiation exceeding 4 W m^{-2} through the snow-albedo feedback."**

- **"To assess the causal impact of TP snow cover, we performed a targeted CESM experiment ($CESM_{TPSC}$) in which surface albedo over the northern TP (86°-94°E, 35°-40°N) was prescribed with a minimum value of 0.8. Surface albedo represents the reflectivity of the land surface, integrating contributions from all surface components including snow, soil, and vegetation. A minimum value of 0.8 was imposed to simulate persistent high snow cover conditions, consistent with the characteristically high reflectivity of snow-dominated surfaces (Cohen and Rind, 1991)."**

- **"Beyond ENSO, we identify that elevated snow cover over the northern TP increases snow albedo and cools the atmospheric column via snow-albedo feedbacks, weakening the subtropical westerly jet and inducing anticyclonic anomalies over northern China."**

The unit in Figure 6a is unclear.

Response:

- We thank the reviewer for pointing this out. Snow albedo is a dimensionless variable ranging from 0 to 1. For better visualization of the relatively small anomalies, the values shown in Fig. 6a were multiplied by 100. We have clarified this in the revised figure caption.

- **"Figure 6.** Anomalies for (a) snow albedo (dimensionless, multiplied by 100)"

Figure 7 is incorrectly referred to as Figure 6 in the text and should be corrected.

Response:

- We appreciate the reviewer's careful reading. The figure citations have been corrected in the revised manuscript:

- **“The cooling effect over TP modulates the meridional temperature gradient and weakens the subtropical westerly jet north of the Plateau (Fig. 7a). Associated with enhanced snow cover, 200-hPa zonal wind speeds are reduced by up to 15 m s^{-1}, inducing an anomalous anticyclonic circulation over northern China (Fig. 7b, c). Under the influence of positive geopotential height anomalies, near-surface wind speeds decrease by more than 0.1 m s^{-1}, and the planetary boundary layer height is reduced by approximately 15 m. These stagnant conditions favor pollutant accumulation, while concurrently elevated surface relative humidity enhances aerosol hygroscopic growth (Fig. 7d), together contributing to increased $PM_{2.5}$ concentrations over northern China.”**